Fully Zwitterionic Diaminobenzoquinonediimines Promoted by Cyanoaromatic N-substituents

Tereza Horáčková, Manon H.E. Bousquet, Adrien Morice, Ugo Triballier, Gabriel Canard, Pavel Lhoták, Denis Jacquemin, Simon Pascal, Olivier Siri

Fully Zwitterionic Diaminobenzoquinonediimines Promoted by Cyanoaromatic N-substituents

Tereza Horáčková,[a,b] Manon H. E. Bousquet,[c] Adrien Morice,[c] Ugo Triballier,[c] Gabriel Canard,[a] Pavel Lhoták,[b] Denis Jacquemin,[c,d,*] Simon Pascal,[a,*] Olivier Siri[a,*]

[a] *Aix Marseille Univ, CNRS UMR 7325, Centre Interdisciplinaire de Nanoscience de Marseille (CINaM), Campus de Luminy, case 913, Marseille cedex 09 13288, France. E-mail: simon.pascal@cnrs.fr; olivier.siri@univ-amu.fr*

[b] *Department of Organic Chemistry, University of Chemistry and Technology, Prague (UCTP), Technická 5, 166 28 Prague 6, Czech Republic.*

[c] *Université de Nantes, CEISAM UMR 6230, CNRS, Nantes F-44000, France. E-mail: Denis.Jacquemin@univ-nantes.fr*

[d] *Institut Universitaire de France (IUF), Paris F-75005, France.*

Abstract

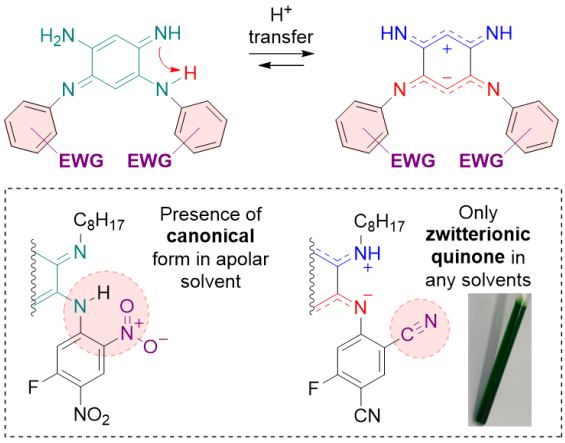

2,5-Diamino-1,4-benzoquinonediimine (DABQDI) derivatives possessing two electron-withdrawing aromatic N-substituents can potentially exhibit a zwitterionic ground state in lieu of the expected canonical structure. It was previously shown that the use of nitroaromatics electron-withdrawing groups (EWG) could yield the quantitative formation of zwitterionic tautomer of DABQDI in polar solvents, while a mixture of canonical and zwitterionic forms was present in low polarity solvents. In this work, we report that the replacement of nitro-containing EWG by weaker nitrile ones prevents the formation of canonical species in apolar solvents for the benefit of the zwitterionic tautomer. This counterintuitive observation is rationalized with theoretical calculations, which points out that the fully zwitterionic electronic structure of the nitrile-containing DABQDI arises from the absence of possible intramolecular hydrogen bonding between the cyanoaromatic N-substituent and the N-H proton of the bridge in the canonical form.

1. Introduction

π-Zwitterions are a class of organic molecules featuring conjugated cationic and anionic charges, providing them with unique electronic and optical properties allowing elaborating new materials for organic electronics and nonlinear optics [1-4]. The design of ground-state π-zwitterions can be rather straightforward when considering squaraine [5-7] and parent zwitterionic polymethines [8-11] that are omnipresent in the fields of photovoltaics, optical detection and bio-imaging. However, expending the diversity of conjugated π-zwitterions is not trivial and only few strategies are emerging in the literature, notably by linking strongly electron-donating and electron-withdrawing groups (EWG) in twisted π-systems [3, 12] or in polycyclic heteroaromatic compounds such as quinacridine derivatives [13, 14], naphthalenediimides [15] and azoniadibenzo[*a*,*j*]phenalenides [16], which often yields photophysical properties in red to near-infrared ranges. Another remarkable strategy towards π-zwitterions is based on the design of rigid polycyclic antiaromatic species that are prompt to form stable ground-state zwitterions (Figure 1), such as tetraphenylhexaazaanthracenes (TPHA) [17-20], tetraazapentacenes (TAP) [21-23] and triazino-phenazine hybrid derivatives [24], bisdithiazoles [25, 26] or benzoquinone dithiazoles (BDT) [27, 28]. Besides, benzoquinone monoimine (BQMI) derivatives are the most simple quinoidal molecules that feature a ground state zwitterionic structure due to the formation of two polymethine subsystems: one trimethine cyanine being positively charged and one negatively charged trimethine oxonol [29-31]. The delocalization of the charges brings to the BQMI unique absorption properties in the visible range, and up to the NIR upon introduction of strong electron-donating N-substituents [32, 33].

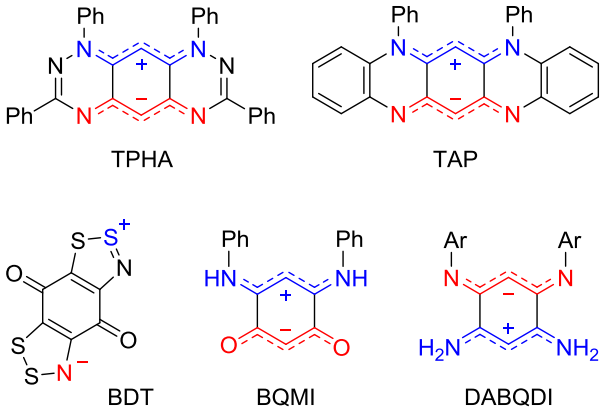

Figure 1. π-zwitterions built around antiaromatic 6-membered rings.

We recently described that 2,5-diamino-1,4-benzoquinonediimines (DABQDI, Figure 1) can adopt either canonical (uncharged) or zwitterionic forms following an intramolecular proton transfer from one 6π-electrons subunit to the other (Figure 2) [34, 35]. Two main parameters can favour the zwitterionic tautomer of DABQDI, namely the presence strong EWG substituents on one of the two trimethine subunits, and a highly polar environment, both parameters logically allowing the easier formation of a charge separated structure. For instance, the introduction of two fluorodinitrobenzene strong EWG in DABQDI **1** (Chart 1) promotes a fully zwitterionic ground state of the quinone in polar solvents only, *e.g.*, dichloromethane, acetone, and dimethylsulfoxide. Nevertheless, when the compound is dissolved in any solvent of lower polarity, a mixture of both canonical and zwitterionic tautomers is formed in solution. While this equilibrium found utility in the development of a colourful vapochromic probe for the detection polar volatile organic compounds [34], further applications of these chromophores, notably in molecular electronics, would require the use of a material exclusively present in its zwitterionic form to guarantee the strong dipole moment that is beneficial for the development of interlayer molecular films in photovoltaic devices and transistors [36-38].

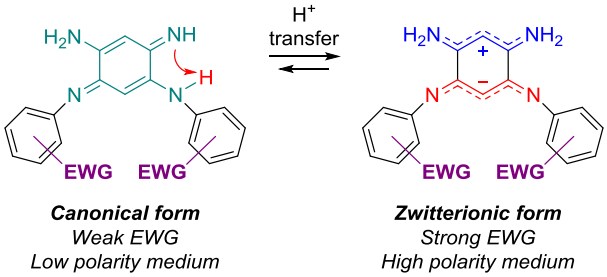

Figure 2. Equilibrium between the canonical and zwitterionic tautomers in 2,5-diamino-1,4-benzoquinonediimines (EWG = electron-withdrawing group).

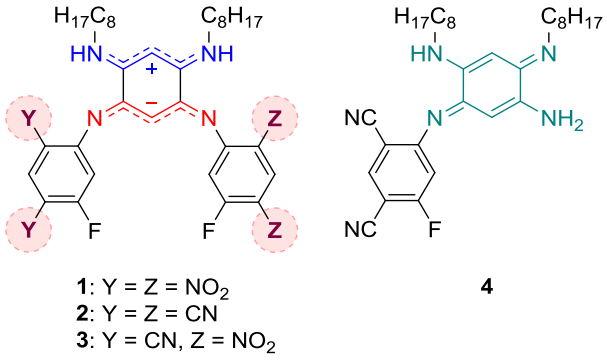

Chart 1. Investigated DABQDIs **1-4**.

For this purpose, we investigate herein the replacement of nitro EWG in the original DABQDI **1** with nitrile functions in the compounds **2-4** (Chart 1). The introduction of the fluoroisophthalonitrile N-substituents impacts the electronic and photophysical properties of the chromophores and promotes the zwitterionic tautomer of quinones **2** and **3** that persists in various solvents, despite the fact that the cyano groups are widely considered as less electron-withdrawing than the nitro ones. These experimental findings are then rationalized through theoretical calculations.

2. Experimental

2.1. Analytical methods and apparatus

The melting points (M.P.) of the vacuum-dried powders were measured in open capillary tubes with a STUART SMP30 melting points apparatus and are uncorrected. NMR spectra were recorded on a JEOL ECS400 NMR spectrometer at room temperature (except when noted otherwise). ^{1}H and ^{13}C NMR chemical shifts are given in ppm (δ) relative to Me_4Si with solvent resonances used as internal standard ($CDCl_3$: 7.26 ppm for ^{1}H and 77.2 for ^{13}C). NMR peak assignments were confirmed using a DEPT-135 method. IR spectra were recorded on an Agilent Cary 630 FTIR equipped with an attenuated total reflectance (ATR) sampling. Electronic absorption spectra were recorded in spectroscopic grade solvents on a VARIAN CARY 50 SCAN spectrophotometer at room temperature with a 300 nm/min scan rate using 1 cm path quartz cuvettes. HRMS analyses were performed on a QStar Elite (Applied Biosystems SCIEX) or a SYNAPT G2 HDMS (Waters) spectrometers by the “Spectropole” of the Aix-Marseille University. These two instruments are equipped with an ESI or MALDI source, and a TOF mass analyzer.

Cyclic voltammetry (CV) data were recorded using a BAS 100 (Bioanalytical Systems) potentiostat and the BAS100W software (v2.3). All experiments were conducted under an argon atmosphere in a standard one-compartment using a three electrodes setup: a Pt working electrode (Ø = 1.6 mm), a Pt counter electrode and a leak-free Ag/AgCl reference electrode of 5 mm diameter. Tetra-*n*-butylammonium hexafluorophosphate ($[^{n}Bu_4][PF_6]$) was used as supporting electrolyte (10^{-1} M), with a concentration of the electro-active compound of *ca*. 10^{-3} M. The reference electrode was calibrated using ferrocene ($E°(Fc/Fc^{+})$ = 0.46V/SCE in DCM) [39]. The scan rate was 100 mV/S. The solution was degassed using argon before recording each

reductive scan, and the working electrode (Pt) was polished before each scan recording.

2.2. Materials and synthetic procedures

Compounds **1** [34], **5** [40], and **6** [41] were prepared following previously reported protocols. All the reactions were carried out under argon atmosphere. Reagents were purchased from Sigma-Aldrich and used as received. When heating was required, oil bathes were used. Column chromatography were performed using Silica 60 M (0.04-0.063 mm).

*Synthesis of **7***. Compounds **5** (100 mg, 0.230 mmol) and **6** (75 mg, 0.457 mmol) were dissolved in 10 mL of anhydrous acetonitrile under argon. The solution was cooled to 0 °C and degassed by argon bubbling for 15 min. Then, *N,N*-diisopropylethylamine (0.24 mL, 1.38 mmol) was added dropwise to the solution at 0 °C. The reaction mixture was then stirred at 25 °C for 30 min and finally heated to reflux overnight. The crude solution was then evaporated under reduced pressure. The residue was purified by column chromatography over silica gel using pure dichloromethane then dichloromethane with 1% of methanol as eluent to afford **7** in 60% yield (90 mg, 0.138 mmol) as a beige solid. **R*f*** = 0.12 (SiO_2, DCM). **M. P.:** 210-212 °C. **^{1}H NMR** (**400 MHz, $CDCl_3$):** δ **=** 7.75 (d, $J_{H\text{-}F}$ = 6.7 Hz, 2H, CH), 6.80 (s, 1H, CH), 6.29 (s, 2H, NH), 6.27 (d, $J_{H\text{-}F}$ = 11.5 Hz, 2H, CH), 5.98 (s, 1H, CH), 3.97 (t, *J* = 5.1 Hz, 2H, NH), 3.18 – 3.13 (m, 4H, NH-CH_2), 1.63 – 1.60 (m, 4H, CH_2), 1.32 – 1.27 (m, 20H, CH_2), 0.89 (t, *J* = 6.9 Hz, 6H, CH_3). **^{13}C{^{1}H} NMR** (**101 MHz, $CDCl_3$):** δ **=** 166.7 (C, $J_{C\text{-}F}$ = 262.8 Hz), 155.2 (C, $J_{C\text{-}F}$ = 13.5 Hz), 146.8 (C), 138.9 (CH, $J_{C\text{-}F}$ = 3.7

Hz), 128.6 (CH), 115.1 (C), 113.1 (C), 109.9 (C), 100.6 (CH, $J_{C\text{-}F}$ = 23.4 Hz), 93.8 (C), 93.2 (CH), 91.6 (C, $J_{C\text{-}F}$ = 18.3 Hz), 43.5 (N-CH_2), 31.9 (CH_2), 29.5 (CH_2), 29.4 (2 CH_2), 27.3 (CH_2), 22.8 (CH_2), 14.3 (CH_3). **IR (neat, cm^{-1}):** ν = 3356, 3240, 3081, 3048, 2923, 2850, 2226, 1632, 1569, 1521, 1449, 1419, 1375, 1323, 1296, 1256, 1215, 1172, 1099, 938, 895, 836, 756, 722, 669. **HRMS (ESI+)** calculated for $[M+H]^+$: 651.3730 ($C_{38}H_{45}F_2N_8^+$), found: 651.3731.

*Synthesis of **10**.* Compounds **5** (270 mg, 0.62 mmol) and **6** (100 mg, 0.609 mmol) were dissolved in 13 mL of anhydrous acetonitrile under argon. The solution was degassed by argon bubbling for 15 min. Then, *N,N*-diisopropylethylamine (0.64 mL, 3.67 mmol) was added dropwise to the solution. The reaction mixture was stirred at 25 °C for 5 min and then heated to reflux for 1.5 h. After the reaction mixture was cooled down to 25 °C, 1,5-difluoro-2,4-dinitrobenzene **9** (120 mg, 0.588 mmol) was added under argon and the reaction was continued at 25 °C overnight. Then, the solvent was evaporated under reduced pressure and the crude product was purified by column chromatography over silica gel using dichloromethane as eluent. The product **10** was isolated in 39% yield (169 mg, 0.245 mmol) as an orange solid. **R*f*** = 0.34 (SiO_2, DCM). **M. P.:** 204-206 °C. **^{1}H NMR** (**400 MHz, $CDCl_3$):** δ = 9.27 (s, 1H, NH), 9.16 (d, $J_{H\text{-}F}$ = 7.8 Hz, 1H, CH), 7.75 (d, $J_{H\text{-}F}$ = 6.8 Hz, 1H, CH), 6.82 (s, 1H, CH), 6.52 (d, $J_{H\text{-}F}$ = 13.2 Hz, 1H, CH), 6.32 (s, 1H, NH), 6.30 (d, $J_{H\text{-}F}$ = 11.2 Hz, 1H, CH), 6.02 (s, 1H, CH), 4.00 (t, *J* = 5.2 Hz, 1H, NH), 3.92 (t, *J* = 5.4 Hz, 1H, NH), 3.19 – 3.15 (m, 4H, NH-*CH_2*), 1.65 – 1.60 (m, 4H, CH_2), 1.33 – 1.27 (m, 20H, CH_2), 0.90 – 0.86 (m, 6H, CH_3). **^{13}C{^{1}H} NMR** (**101 MHz, $CDCl_3$):** δ = 166.7 (C, $J_{C\text{-}F}$ = 264.8 Hz), 160.0 (C, $J_{C\text{-}F}$ = 272.5 Hz), 155.1 (C, $J_{C\text{-}F}$ = 14.1 Hz), 150.1 (C, $J_{C\text{-}F}$ = 14.1 Hz), 146.8 (C), 146.1 (C), 138.9 (CH), 128.2 (CH), 128.0 (C), 127.9 (CH), 127.4 (C, $J_{C\text{-}F}$ = 9.7

Hz), 115.1 (C), 113.0 (C), 110.1 (C), 109.6 (C), 103.8 (CH, $J_{C\text{-}F}$ = 30.2 Hz), 100.6 (CH, $J_{C\text{-}F}$ = 30.2 Hz), 93.9 (C), 93.3 (CH), 91.6 (C, $J_{C\text{-}F}$ = 19.7 Hz), 43.61 (N-CH_2), 43.55 (N-CH_2), 31.9 (CH_2), 29.44 (CH_2), 29.36 (CH_2), 27.3 (CH_2), 22.8 (CH_2), 14.2 (CH_3). **IR (neat, cm^{-1}):** ν = 3362, 3267, 3049, 2924, 2853, 2232, 2110, 1634, 1624, 1580, 1524, 1480, 1454, 1413, 1375, 1334, 1296, 1261, 1215, 1169, 1127, 1054, 938, 877, 836, 742, 713, 691, 671. **HRMS (ESI+)** calculated for $[M+H]^+$: 691.3526 ($C_{36}H_{45}N_8O_4F_2^+$), found: 691.3526.

*Synthesis of **2**.* Compound **7** (30 mg, 0.046 mmol) was dissolved in 1 mL of degassed chloroform and *p*-chloranil (12 mg, 0.049 mmol) was added to the solution. After the reaction mixture was stirred at 25 °C for 30 min, the solvent was evaporated under reduced pressure. The crude product was purified by column chromatography over silica gel using pure dichloromethane as eluent, affording compound **2** in 78% yield (23.3 mg, 0.036 mmol) as a dark green solid. **R*f*** = 0.13 (SiO_2, DCM). **M. P.:** 183-185 °C. **^{1}H NMR** (**400 MHz, $CDCl_3$):** δ = 8.64 (br s, 2H, NH), 7.82 (d, $J_{H\text{-}F}$ = 7.1 Hz, 2H, CH), 6.86 (d, $J_{H\text{-}F}$ = 11.1 Hz, 2H, CH), 5.46 (s, 1H, CH), 5.36 (s, 1H, CH), 3.43 (t, *J* = 7.2 Hz, 4H, N-CH_2), 1.84 – 1.77 (m, 4H, CH_2), 1.49 – 1.43 (m, 4H, CH_2), 1.35 – 1.25 (m, 16H, CH_2), 0.90 – 0.86 (m, 6H, CH_3). **^{13}C{^{1}H} NMR** (**101 MHz, $CDCl_3$):** δ = 165.5 (C, $J_{C\text{-}F}$ = 266.5 Hz), 159.2 (C, $J_{C\text{-}F}$ = 10.3 Hz), 157.7 (C), 150.2 (C), 138.7 (CH, $J_{C\text{-}F}$ = 3.4 Hz), 115.99 (C), 113.1 (C), 108.8 (CH, $J_{C\text{-}F}$ = 20.5 Hz), 105.2 (C, $J_{C\text{-}F}$ = 2.03 Hz), 95.1 (C, $J_{C\text{-}F}$ = 18.10 Hz), 86.53 (CH), 83.46 (CH), 43.9 (N-CH_2), 31.9 (CH_2), 29.24 (CH_2), 29.19 (CH_2), 28.3 (CH_2), 27.1 (CH_2), 22.7 (CH_2), 14.2 (CH_3). **IR (neat, cm^{-1}):** ν = 3367, 3277, 3226, 2923, 2853, 2579, 2223, 1606, 1591, 1545, 1503, 1453, 1421, 1329, 1290, 1268, 1230, 1146, 1087,

1052, 908, 839, 811, 757, 674. **HRMS (ESI+)** calculated for $[M+H]^+$: 649.3573 ($C_{38}H_{43}N_8F_2^+$), found: 649.3570.

*Synthesis of **3***. Compound **10** (20 mg, 0.029 mmol) was dissolved in 1 mL of degassed chloroform and *p*-chloranil (16 mg, 0.066 mmol) was added to the solution. After the reaction mixture was stirred at 25 °C for 30 min, the solvent was evaporated under reduced pressure. The crude product was purified by preparative thin layer chromatography over silica gel using dichloromethane as eluent to afford **3** in 91% yield (18.1 mg, 0.026 mmol) as a dark green solid. **R*f*** = 0.34 (SiO_2, DCM). **M. P.:** 114-116 °C. **^{1}H NMR** (**400 MHz, $CDCl_3$):** δ = 8.82 (d, $J_{H\text{-}F}$ = 7.8 Hz, 1H, CH), 8.56 (br s, 2H, NH), 7.82 (d, $J_{H\text{-}F}$ = 6.9 Hz, 1H, CH), 6.94 (d, $J_{H\text{-}F}$ = 12.1 Hz, 1H, CH), 6.82 (d, $J_{H\text{-}F}$ = 10.5 Hz, 1H, CH), 5.39 (s, 1H, CH), 5.38 (s, 1H, CH), 3.46 – 3.40 (m, 4H, N-CH_2), 1.84 – 1.77 (m, 4H, CH_2), 1.46 – 1.25 (m, 20H, CH_2), 0.90 – 0.87 (m, 6H, CH_3). **^{13}C{^{1}H} NMR** (**101 MHz, $CDCl_3$):** δ = 165.5 (C, $J_{C\text{-}F}$ = 267.4 Hz), 159.1 (C, $J_{C\text{-}F}$ = 10.6 Hz), 158.3 (C, $J_{C\text{-}F}$ = 272.5 Hz), 157.1 (C, $J_{C\text{-}F}$ = 12.7 Hz), 151.6 (C, $J_{C\text{-}F}$ = 11.5 Hz), 150.3 (C), 149.6 (C), 140.95 (C), 138.7 (CH, $J_{C\text{-}F}$ = 2.8 Hz), 137.8 (C), 130.1 (C), 125.5 (CH), 115.9 (C), 113.1 (C), 111.5 (CH, $J_{C\text{-}F}$ = 23.3 Hz), 108.8 (CH, $J_{C\text{-}F}$ = 20.3 Hz), 104.9 (C), 95.3 (C, $J_{C\text{-}F}$ = 17.9 Hz), 87.0 (CH), 83.7 (CH), 44.4 (N-CH_2), 43.9 (N-CH_2), 31.9 (CH_2), 29.8 (CH_2), 29.3 (CH_2), 29.2 (CH_2), 28.5 (CH_2), 28.4 (CH_2), 27.1 (CH_2), 22.8 (CH_2), 14.2 (CH_3). It is envisageable that four CH_2 signals are overlapped or equivalent with other CH_2 signals in the 32 – 22 ppm region, as this is the case for the second CH_3 signal. **IR (neat, cm^{-1}):** ν = 3292, 3102, 2922, 2853, 2323, 2220, 1610, 1588, 1503, 1456, 1404, 1379, 1324, 1288, 1210, 1147, 1124, 1083, 1043, 910, 882, 830, 795, 759, 701, 676. **HRMS (ESI+)** calculated for $[M+H]^+$: 689.3370 ($C_{36}H_{43}N_8O_4F_2^+$), found: 689.3369.

*Synthesis of **4**.* Compounds **5** (270 mg, 0.620 mmol) and **6** (100 mg, 0.609 mmol) were dissolved in 17 mL of anhydrous acetonitrile under argon. The solution was degassed by argon bubbling for 15 min. Then, *N,N*-diisopropylethylamine (0.63 mL, 3.62 mmol) was added dropwise to the solution. The reaction mixture was stirred at 25 °C for 5 min and then heated to reflux for 1.5 h. After the reaction mixture was cooled down to 25 °C, the solvent was then evaporated under reduced pressure. The crude residue was purified by column chromatography over silica gel using dichloromethane with 1% of methanol as eluent to afford **4** in 28% yield (85.4 mg, 0.169 mmol) as a brown solid. **R*f*** = 0.21 (SiO_2, DCM/MeOH, 99/1). **M. P.:** 123-125 °C. **^{1}H NMR** (**400 MHz, $CDCl_3$):** δ **=** 7.88 (d, $J_{H\text{-}F}$ = 6.8 Hz, 1H, CH), 6.82 (d, $J_{H\text{-}F}$ = 10.0 Hz, 1H, CH), 5.98 (br s, 1H, NH), 5.35 (s, 1H, CH), 5.20 (s, 1H, CH), 3.50 (t, *J* = 6.9 Hz, 4H, N-CH_2), 3.10 (t, *J* = 7.2 Hz, 4H, N-CH_2), 1.75 – 1.65 (m, 4H, CH_2), 1.42 – 1.25 (m, 20H, CH_2), 0.90 – 0.86 (m, 6H, CH_3). **^{13}C{^{1}H} NMR** (**101 MHz, $CDCl_3$):** δ **=** 165.2 (C, $J_{C\text{-}F}$ = 267.5 Hz), 161.1 (C, $J_{C\text{-}F}$ = 10.5 Hz), 157.33 (C, $J_{C\text{-}F}$ = 7.9 Hz), 157.31 (C), 153.1 (C, $J_{C\text{-}F}$ = 3.3 Hz), 152.2 (C), 138.7 (CH), 115.1 (C), 112.9 (C), 109.9 (CH, $J_{C\text{-}F}$ = 21.5 Hz), 103.9 (C), 96.3 (C, $J_{C\text{-}F}$ = 17.3 Hz), 89.5 (CH), 86.2 (CH), 50.7 (N-CH_2), 43.0 (CH_2), 32.0 (CH_2), 31.9 (CH_2), 29.8 (CH_2), 29.6 (CH_2), 29.5 (CH_2), 29.4 (CH_2), 29.3 (CH_2), 28.5 (CH_2), 27.8 (CH_2), 27.3 (CH_2), 22.8 (CH_2), 22.8 (CH_2), 14.3 (CH_3), 14.2 (CH_3). **IR (neat, cm^{-1}):** v = 3438, 3329, 3047, 2917, 2849, 2233, 2112, 1625, 1602, 1562, 1535, 1511, 1466, 1409, 1363, 1331, 1289, 1267, 1220, 1150, 1085, 992, 925, 900, 867, 808, 786, 750, 722, 656. **HRMS (ESI+)** calculated for $[M+H]^+$: 505.3450 ($C_{30}H_{42}FN_6^+$), found: 505.3452.

2.3. Theoretical calculations

All calculations have been carried out on structures using methyl groups instead of the longer alkyl chains and have been performed with Gaussian16 [42], using default procedures and algorithms except when noted below. We have selected the PBE0 [43] global hybrid functional for the ground-state calculations, and applied tighten thresholds for the energy (at least 10^{-9} au) and geometry convergences (so-called *tight* threshold in Gaussian), as well as used an improved DFT integration grid (*ultrafine* grid). For all compounds, the ground-state forces were minimized with the 6-31G(d) (for early conformational screening) and 6-311++G(2d,2p) (for the presented results on the key structures) atomic basis sets. We subsequently verified the absence of imaginary frequencies by computing analytically the Hessian at the same level of theory. The excited-state calculations were performed with Time-Dependent Density Functional Theory (TD-DFT) considering 5-to-15 states determined with the CAM-B3LYP long-range corrected functional [44] (more suited for charge-transfer states) and the same 6-311++G(2d,2p) atomic basis set. The solvent effects were modeled through the Polarizable Continuum Model (PCM) [45], using the linear-response *non-equilibrium* model for the excited-state calculations. The density difference plots representing the excited states have been drawn by computing the excited state density with the *Z*-vector approach. Charge-transfer parameters were determined using Le Bahers' model as implemented in Gaussian16 – relaxed excited-state densities have been used [46].

3. RESULTS AND DISCUSSION

3.1. Synthesis

The syntheses of the nitrile-containing targets were carried out *via* nucleophilic aromatic substitution of tetraaminobenzene (**5**) on 4,6-difluoroisophthalonitrile (**6**) in refluxing acetonitrile (Scheme 1). When one equivalent of **5** and two equivalents of **6** were used, the intermediate **7** was isolated in 60% yield after purification by silica gel column chromatography. To reach the hybrid compound **10** substituted with both nitrile- and nitro-containing aromatics, the synthesis of the intermediate **8** was envisaged following the reaction of equimolar quantities of **5** and **6**. However, as a result of the spontaneous aerobic oxidation of **8** during the reaction workup, the quinone **4** was isolated as a brown solid, the structure of which was confirmed by the high-resolution mass spectrum analysis that shows molecular ion peak with *m/z* 505.3452, corresponding to [**4**+H]$^+$. It is noteworthy that such [1+1] substitution adduct was rarely isolated previously using 1,5-difluoro-2,4-dinitrobenzene **9** as electrophile, notably due to the intramolecular NH$^{\cdots}$O$_2$N bonds strongly favouring the [1+2] adduct (the aromatic precursor of **1**) [47]. The poor stability of **4** regarding oxidation was also previously noticed for tetraaminobenzene derivatives substituted with weak electron-withdrawing aromatics [34, 48]. This observation is easily explained by the presence of a single fluoroisophthalonitrile moiety in **8** compared to the presence of two similar substituents in the more stable **7**. Consequently, the synthesis of **10** was undertaken without isolation of **8**, following a two steps in one pot strategy that afforded **10** in a moderate 39% yield, the first substitution being the limiting step. Attempts to promote the nucleophilic aromatic substitution by increasing the reaction time or changing the temperature did not improve the yield of **10**. Finally, compounds **7** and **10** were readily oxidized in presence of two equivalents of *p*-chloranil to afford the quinones **2** and **3** in 78% and 91% yields,

respectively, the green coloration of their powders indicating the presence of zwitterionic species (*vide infra*).

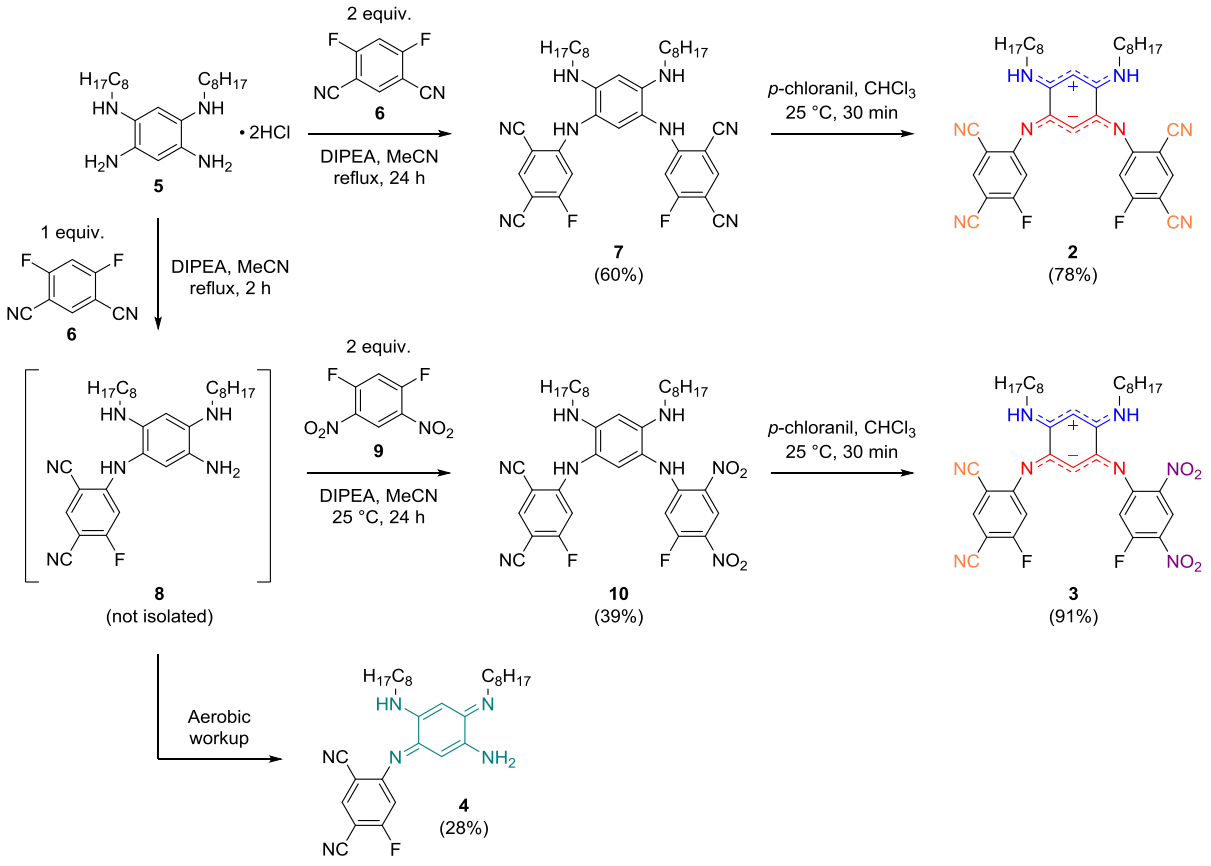

Scheme 1. Synthesis of quinones **2-4**.

3.2. Electronic properties

The cyclic voltammograms of **1-4** were recorded in DCM and show irreversible first reduction processes at -0.84, -0.90 and -0.99 V *vs.* Fc/Fc^{+}, for compounds **1**, **3** and **2**, respectively (Figure 3 and Table 1). This order follows the decrease in the electron-withdrawing strength of the N-substituents, the reduction being facilitated for the nitro-containing species. In this series, the oxidation waves are poorly shifted compared to **1**, nevertheless reversible processes are found at *ca*. 0.68 V upon introduction of nitrile functions in **2** and **3**, instead of the irreversible process

observed for **1**. The quinone **4** exhibits irreversible processes, the reduction and oxidation waves are respectively found at -1.29 and 0.49 V, suggesting a canonical tautomer, by comparison with the previously reported 1,3-bis(trifluoromethyl)benzene-containing DABQDI derivative featuring a canonical ground state and irreversible redox processes found at -1.29 and 0.44 V Fc/Fc^+ in the same solvent [34].

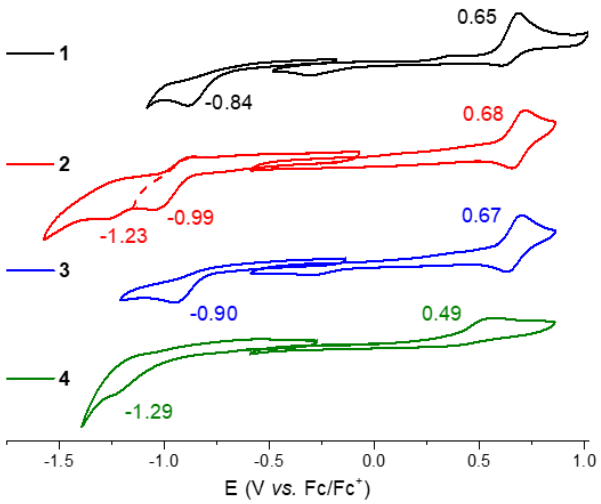

Figure 3. Cyclic voltammograms of compounds **1-4** in DCM solutions containing 0.1 M of [^{n}Bu$_4$N][PF$_6$].

Table 1. Summary of the half-wave or peak potentials (V *vs*. Fc/Fc^+) of the compounds **1-4** (recorded in dichloromethane solutions containing 0.1 M of [^{n}Bu$_4$N][PF$_6$] at a scan rate of 100 mV s^{-1}) and their longest wavelength of maximal absorption with the related molar extinction coefficients, recorded in dichloromethane (DCM) and toluene (PhMe) solutions.

Dye	Reduction		Oxidation	ΔE (V)[a]	λ_{max} (nm) (ε ($M^{-1}.cm^{-1}$))
	$E_{1/2}$ red$_2$	$E_{1/2}$ red$_1$	$E_{1/2}$ ox		
1	-	–0.84[b]	0.65[b]	1.48	DCM: 697 (6850) PhMe: 705 (2410)
2	–1.23[b]	–0.99 (126)[c]	0.68 (62)[c]	1.67	DCM: 697 (7680) PhMe: 713 (7320)
3		–0.90[b]	0.67 (71)[c]	1.57	DCM: 698 (5300)

				PhMe: 704 (3360)
4	–1.29[b]	0.49[b]	1.78	DCM: 362 (17630) PhMe: 364 (15860)

[a]Electrochemical gap: $\Delta E = E_{1/2}(ox) - E_{1/2}(red_1)$ or $\Delta E = E_{pa}(ox) - E1/2(red_1)$. [b]Irreversible peak potential at a scan rate of 100 mV s^{-1}. [c]$\Delta E = E_{pa} - E_{pc}$ expressed in mV.

When the two tautomers are close in energy, the canonical-zwitterionic equilibrium is impacted by the polarity of the environment in both solution and solid states [34, 35]: the more polar the medium is, the more intense the band centred at 700 nm is. This low energy hallmark transition is attributed to an intramolecular charge-transfer (ICT) between the negatively and positively charged moieties of the zwitterionic tautomer and any intensity increase observed on this band while increasing the solvent polarity implies an increasing proportion of the zwitterionic species, as illustrated with nitro-containing quinone **1** in Figure 4. Indeed, while increasing the solvent polarity, the lowest energy band of **1** undergoes a significant hyperchromic effect, with ε^{705} ~ 2400 $M^{-1}.cm^{-1}$ in toluene and ε^{697} ~ 6900 $M^{-1}.cm^{-1}$ in DCM. Surprisingly, such shift is not observed for the nitrile-containing quinone **2** with ε *ca*. 7500 $M^{-1}.cm^{-1}$ in these two solvents, apparently indicating the exclusive presence of the zwitterionic tautomer in solution in all solvents. This hints that the canonical tautomer is significantly less stable in **2** than **1**, which might look counterintuitive as the nitro accepting strength exceeds its nitrile counterpart [49], and one would naively foresee the opposite behaviour, as the strongest acceptors should, in principle, stabilize the charge-separated zwitterionic isomer. Less surprisingly, **3** featuring mixed nitrile and nitro EWG exhibits an intermediate behaviour, the lowest energy band intensity varying between 3400-5300 $M^{-1}.cm^{-1}$, going from toluene to DCM. The spectrum of compound **4** does not show any band centred at 700 nm but

a broad and weak shoulder between 500-700 nm, which indicates the predominance of the canonical form in solution irrespective of the solvent. This observation is in line with the brown powder coloration of **4** and the cyclic voltammogram of this compound that notably differs from the ones recorded for the ground state zwitterions **1-3**. Nevertheless, the slight bathochromic shift of the lower energy band observed in DMSO (ε^{600} ~ 800 $M^{-1}.cm^{-1}$) could be attributed to the presence of a trifling portion of zwitterion. Finally, we note that the pH-dependent absorption properties of the quinones **2-4** revealed the possibility to generate cationic and anionic quinones in solution, as previously reported [34] (see Supporting Information for details).

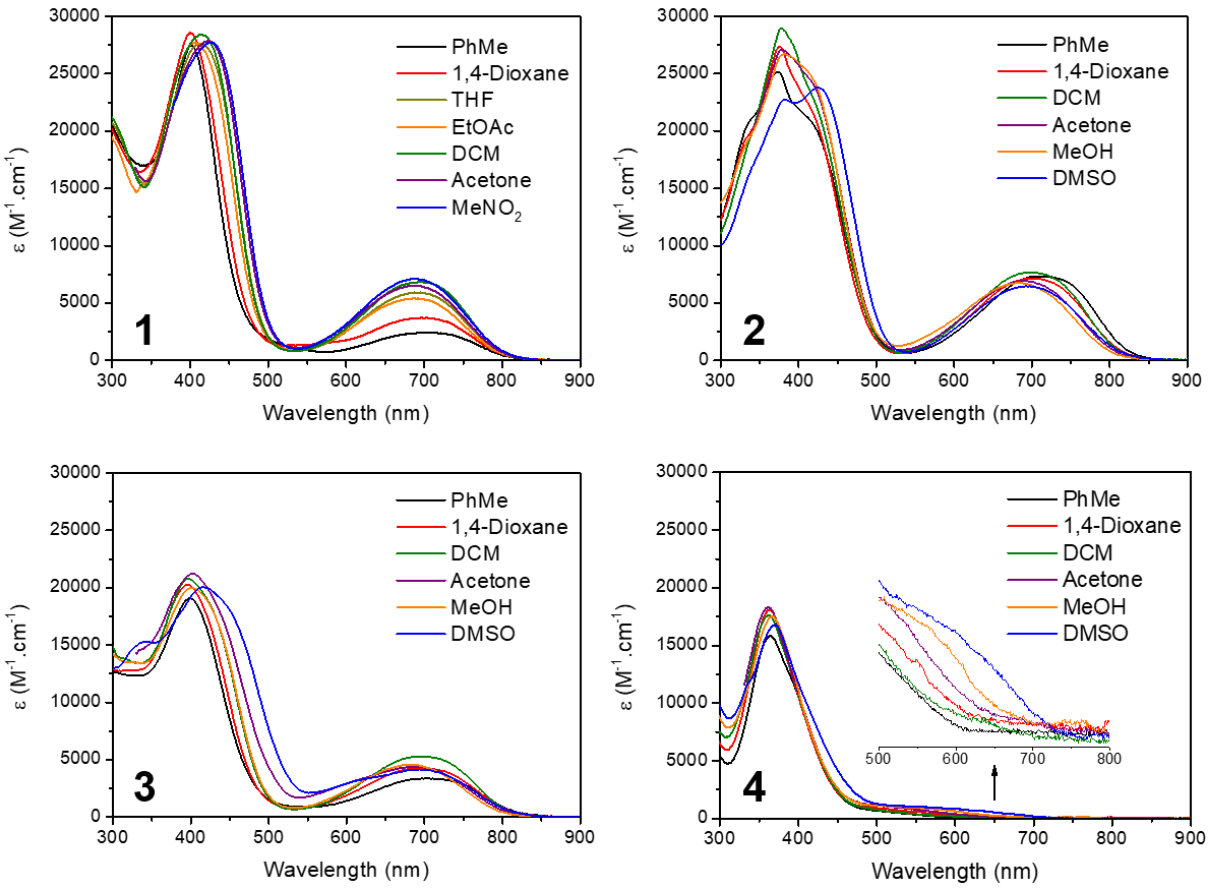

Figure 4. Electronic absorption solvatochromism of compounds **1-4** (*ca*. 10^{-5} M).

To specifically assess the impact of the N-substituents, the electronic absorptions of **1-4** were compared in the least polar solvent (Figure 5). The quinone **4** only presents the canonical tautomer in toluene, the fluoroisophthalonitrile moiety being insufficiently electron-withdrawing to promote the zwitterionic form. In contrast, compounds **1-3** present the zwitterion signature in the red region and, surprisingly, the intensity of the band is sensibly increased upon replacement of the nitro functions by the nitrile ones. As stated above, such result is unexpected since the stronger electron-withdrawing nitroaromatic substituents would be expected to more efficiently promote fully zwitterionic species compared to the cyanoaromatic ones. To study the influence of the nitrile and nitro moieties on the canonical-zwitterionic equilibrium in more details, it was deemed necessary to carry out an *in silico* investigation.

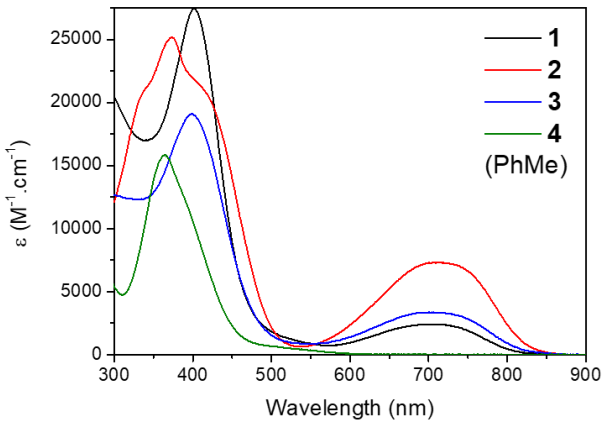

Figure 5. Comparison of the electronic absorption of compounds **1-4** in toluene.

3.3. Theoretical study

To obtain more insights into the experimental results, we have carried out theoretical calculations using DFT and TD-DFT, with a methodology detailed in the experimental section. This approach was used before for similar species [34, 35]. One key aspect here is the energetic balance between the canonical and zwitterionic

tautomers (Figure 2). Of course, DFT is not infinitely accurate with typical errors on relative free energies of similar species of *ca*. 1-3 kcal.mol^{-1} (which can lead to significant changes in Boltzmann populations). Nevertheless, we do trust that the trends in the series are correct. All our results are detailed in the SI and we focus here on the main aspects helping to grasp the unexpected measurements. First, for all structures TD-DFT calculations clearly confirm that the presence of the redshifted absorption at *ca*. 700 nm experimentally is a signature of the zwitterionic tautomer, none of the canonical forms absorbing in that region (see the SI).

We have already considered **1** in a previous work [35], so we can likely be brief. In toluene and DMSO we found that the most stable zwitterionic structure is stabilized by 2.9 and 5.0 kcal.mol^{-1} as compared to its canonical counterpart. Considering the above-state error bar, this indicates that the zwitterion is almost exclusively present in DMSO, whereas a small portion of canonical tautomer is present in toluene. This is qualitatively consistent with the experimental spectrum displayed in Figure 4, which shows that the characteristic zwitterionic band is significantly more intense in the most polar solvents.

For **2**, we performed a complete conformational search for both tautomeric forms. In DMSO, the difference of free energies between the most stable zwitterion and canonical structures attains 6.8 kcal.mol^{-1}. The corresponding difference is 4.6 kcal.mol^{-1} in toluene. In other words, the zwitterionic tautomer is even more stabilized than in **1**. This theoretical prediction fits experiment, as Figure 4 clearly suggests that the zwitterion is systematically present in **2** irrespective of the solvent, indicating that it is strongly favoured. However, as evoked previously, this result is surprising since the strongest accepting group *(i.e.*, the nitro) should normally ease the formation of the charge-separated structure (*i.e.*, the zwitterion) in the ground electronic state, so

one would expect the canonical form to become relatively more stabilized in **2** than in **1**. By examining the actual geometries predicted by DFT, we could rationalize this outcome. Indeed, as can be seen in Figure 6, in the canonical form of **1**, a bifurcated hydrogen bond absent in the zwitterion is present [50, 51], as the transferred hydrogen atom is in close contact with one of the oxygen atom of the vicinal *ortho* nitro group. Such interaction is absent in **2**, where the transferred hydrogen atom is more than 2.8 Å away from the nitrogen atom of the cyano group. This extra stabilizing interaction, counterbalancing the purely electronic effect, is present in **1** but absent in **2**, which likely explains why the formation of the canonical structure can be observed in the former compound and not the latter.

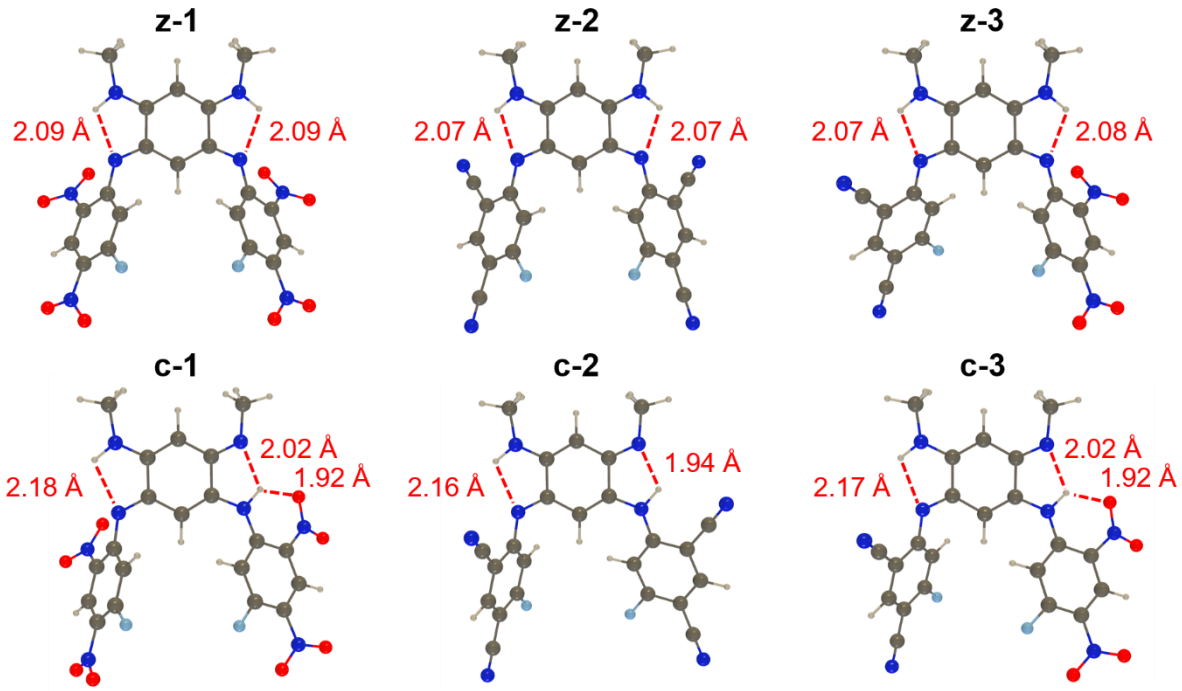

Figure 6. DFT structures of the most stable conformers of the zwitterionic (top) and canonical (bottom) tautomers of **1**, **2**, and **3** (from left to right) in DMSO. Significant hydrogen bonds (Å) are indicated. In the canonical **2**, the shortest distance between the (transferred) hydrogen atom and the nitrogen of the cyano group is 2.86 Å.

This analysis is further strengthened by the results obtained for **3** (see the SI for details). Indeed, on the one hand, the most stable canonical form displays a hydrogen atom on the nitro side (the transfer on the nitrile side leads to a structure less stable by 0.7 kcal.mol^{-1}), and, on the other hand, this structure is less stable than its zwitterionic counterpart by only 4.6 (2.6) kcal.mol^{-1}. These values are very similar to the one found for **1**, hinting that **3** and **1** should have similar behaviour, which is indeed clear from Figure 5. Considering all computed conformers, this leads to a slight presence of the canonical form in the apolar solvent (see the SI).

Finally for **4**, theory predicts a 98/2 (99/1) canonical/zwitterion blend in neutral DMSO (DCM), the predominance of the canonical tautomer being a logical consequence of the presence of only two accepting groups instead of four. As for the other compounds, TD-DFT predicts that the zwitterionic lowest absorption is both (much) more intense and redshifted as compared to the canonical one (see the SI), and therefore, the very weak absorption above 600 nm in the experimental measurements (Figure 4) is a signature of a tiny presence of zwitterion in the solution.

4. CONCLUSION

The synthesis of fluoroisophthalonitrile-containing DABQDIs was achieved and their spectroscopic properties revealed a fully zwitterionic structure in solution for **2** and, to a lesser extent, for the hybrid nitro/cyano compound **3**, while the fluorodinitrobenzene-containing analogue **1** showed the presence of a mixture of zwitterionic and canonical species in solution. These results are counterintuitive at first glance since nitro EWG are stronger acceptor than cyano groups, the former should promote to a greater extent the zwitterionic tautomer. However, the

computational study brings evidences that, while there is a possible interaction between the transferrable hydrogen atom of the quinone and the oxygen atom of the closest nitro function that relatively stabilises the canonical form in **1**, the fully zwitterionic electronic structure of **2** arises from the absence of intramolecular hydrogen bonding between the closest nitrile group and the transferred H atom (*i.e.* absence of bifurcated H-bonding interactions). These results bring evidences that the use of cyanoaromatic EWG is relevant for the future design of stable and fully zwitterionic DABQDI-based architectures such as azacalixquinarene macrocycles.

CRediT authorship contribution statement

Tereza Horáčková: Investigation, Validation, Writing - Review & Editing. **Manon H. E. Bousquet:** Investigation, Validation, Writing - Review & Editing. **Adrien Morice:** Investigation, Validation. **Ugo Triballier:** Investigation, Validation. **Gabriel Canard:** Investigation, Validation, Writing - Review & Editing. **Pavel Lhoták:** Validation, Supervision, Writing - Review & Editing. **Denis Jacquemin:** Conceptualization, Validation, Investigation, Writing - Review & Editing, Supervision. **Simon Pascal:** Conceptualization, Validation, Investigation, Writing - Original Draft, Writing - Review & Editing, Visualization, Supervision. **Olivier Siri:** Conceptualization, Validation, Writing - Review & Editing, Supervision.

Declaration of competing interest

The authors declare that they have no known competing financial interests or personal relationships that could have appeared to influence the work reported in this paper.

Acknowledgements

This work was supported from the grant of Specific university research – grant no. A2 FCHT 2022 098, and by the Agence Nationale de la Recherche, in the frame of the SOCOOL project. We acknowledge the Centre National de la Recherche Scientifique and the ministère de l'enseignement supérieur et de la recherche. P.L. thanks the Czech Science Foundation (20-08667S) for financial support. This work used the computational resources of the GliCid/CCIPL computational *mesocenter* installed in Nantes.

Appendix A. Supplementary data

Supplementary data to this article can be found online at xxx.

References

[1] Zheng Y, Wudl F. Organic spin transporting materials: present and future. J Mater Chem A. 2014;2(1):48-57.
[2] Beverina L, Pagani GA. π-Conjugated Zwitterions as Paradigm of Donor–Acceptor Building Blocks in Organic-Based Materials. Acc Chem Res. 2014;47(2):319-29.
[3] Lou AJT, Marks TJ. A Twist on Nonlinear Optics: Understanding the Unique Response of π-Twisted Chromophores. Acc Chem Res. 2019;52(5):1428-38.
[4] Pascal S, David S, Andraud C, Maury O. Near-infrared dyes for two-photon absorption in the short-wavelength infrared: strategies towards optical power limiting. Chem Soc Rev. 2021;50(11):6613-58.
[5] Chen G, Sasabe H, Igarashi T, Hong Z, Kido J. Squaraine dyes for organic photovoltaic cells. J Mater Chem A. 2015;3(28):14517-34.
[6] Ilina K, MacCuaig WM, Laramie M, Jeouty JN, McNally LR, Henary M. Squaraine Dyes: Molecular Design for Different Applications and Remaining Challenges. Bioconjugate Chem. 2020;31(2):194-213.
[7] He J, Jo YJ, Sun X, Qiao W, Ok J, Kim T-i, et al. Squaraine Dyes for Photovoltaic and Biomedical Applications. Adv Funct Mater. 2021;31(12):2008201.
[8] Zheng Y, Miao M-S, Zhang Y, Nguyen T-Q, Wudl F. Striking Effect of Intra- versus Intermolecular Hydrogen Bonding on Zwitterions: Physical and Electronic Properties. J Am Chem Soc. 2014;136(33):11614-7.
[9] Lynch DE, Hamilton DG. Croconaine Dyes – the Lesser Known Siblings of Squaraines. Eur J Org Chem. 2017;2017(27):3897-911.
[10] Nagao Y, Sakai T, Kozawa K, Urano T. Synthesis and properties of barbiturate indolenine heptamethinecyanine dyes. Dyes Pigm. 2007;73(3):344-52.
[11] Taylor D, Hu X, Wu C-M, Tobin JM, Oriou Z, He J, et al. Superprotonic conduction of intrinsically zwitterionic microporous polymers based on easy-to-make squaraine, croconaine and rhodizaine dyes. Nanoscale Adv. 2022;4(13):2922-8.

[12] Shimizu A, Ishizaki Y, Horiuchi S, Hirose T, Matsuda K, Sato H, et al. HOMO–LUMO Energy-Gap Tuning of π-Conjugated Zwitterions Composed of Electron-Donating Anion and Electron-Accepting Cation. J Org Chem. 2021;86(1):770-81.
[13] Pascal S, Besnard C, Zinna F, Di Bari L, Le Guennic B, Jacquemin D, et al. Zwitterionic [4]helicene: a water-soluble and reversible pH-triggered ECD/CPL chiroptical switch in the UV and red spectral regions. Org Biomol Chem. 2016;14(20):4590-4.
[14] Delgado IH, Pascal S, Besnard C, Voci S, Bouffier L, Sojic N, et al. C-Functionalized Cationic Diazaoxatriangulenes: Late-Stage Synthesis and Tuning of Physicochemical Properties. Chem Eur J. 2018;24(40):10186-95.
[15] Kumar S, Shukla J, Mandal K, Kumar Y, Prakash R, Ram P, et al. Doubly zwitterionic, di-reduced, highly electron-rich, air-stable naphthalenediimides: redox-switchable islands of aromatic–antiaromatic states. Chem Sci. 2019;10(26):6482-93.
[16] Arikawa S, Shimizu A, Shintani R. Azoniadibenzo[a,j]phenalenide: A Polycyclic Zwitterion with Singlet Biradical Character. Angew Chem Int Ed. 2019;58(19):6415-9.
[17] Hutchison K, Srdanov G, Hicks R, Yu H, Wudl F, Strassner T, et al. Tetraphenylhexaazaanthracene: A Case for Dominance of Cyanine Ion Stabilization Overwhelming 16π Antiaromaticity. J Am Chem Soc. 1998;120(12):2989-90.
[18] Langer P, Bodtke A, Saleh NNR, Görls H, Schreiner PR. 3,5,7,9-Tetraphenylhexaazaacridine: A Highly Stable, Weakly Antiaromatic Species with 16 π Electrons. Angew Chem Int Ed. 2005;44(33):5255-9.
[19] Constantinides CP, Zissimou GA, Berezin AA, Ioannou TA, Manoli M, Tsokkou D, et al. Tetraphenylhexaazaanthracenes: 16π Weakly Antiaromatic Species with Singlet Ground States. Org Lett. 2015;17(16):4026-9.
[20] Zissimou GA, Constantinides CP, Manoli M, Pieridou GK, Hayes SC, Koutentis PA. Oxidation of Tetraphenylhexaazaanthracene: Accessing a Scissor Dimer of a 16π Biscyanine. Org Lett. 2016;18(5):1116-9.
[21] Wudl F, Koutentis PA, Weitz A, Ma B, Strassner T, Houk KN, et al. Polyazaacenes: new tricks for old dogs. Pure Appl Chem. 1999;71(2):295-302.
[22] Koutentis PA. Regiospecific synthesis of 5,7-disubstituted quinoxalino[2,3-*b*]phenazines. ARKIVOC. 2002;2002(6):175-91.
[23] Guevara-Level P, Pascal S, Siri O, Jacquemin D. First principles investigation of the spectral properties of neutral, zwitterionic, and bis-cationic azaacenes. Phys Chem Chem Phys. 2019;21(41):22910-8.
[24] Ioannou TA, Koutentis PA, Krassos H, Loizou G, Re DL. Some cyclization reactions of 1,3-diphenylbenzo[e][1,2,4]triazin-7(1H)-one: preparation and computational analysis of non symmetrical zwitterionic biscyanines. Org Biomol Chem. 2012;10(7):1339-48.
[25] Beer L, Oakley RT, Mingie JR, Preuss KE, Taylor NJ, Cordes AW. Antiaromatic Bis(1,2,3-dithiazoles) with Zwitterionic Ground States. J Am Chem Soc. 2000;122(31):7602-3.
[26] Winter SM, Roberts RJ, Mailman A, Cvrkalj K, Assoud A, Oakley RT. Thermal conversion of a pyridine-bridged bisdithiazolyl radical to a zwitterionic bisdithiazolopyridone. Chem Commun. 2010;46(25):4496-8.
[27] Mailman A, Leitch AA, Yong W, Steven E, Winter SM, Claridge RCM, et al. The Power of Packing: Metallization of an Organic Semiconductor. J Am Chem Soc. 2017;139(6):2180-3.
[28] Lekin K, Leitch AA, Assoud A, Yong W, Desmarais J, Tse JS, et al. Benzoquinone-Bridged Heterocyclic Zwitterions as Building Blocks for Molecular Semiconductors and Metals. Inorg Chem. 2018;57(8):4757-70.
[29] Siri O, Braunstein P. Unprecedented zwitterion in quinonoid chemistry. Chem Commun. 2002(3):208-9.
[30] Braunstein P, Siri O, Taquet J-P, Rohmer M-M, Bénard M, Welter R. A 6π + 6π Potentially Antiaromatic Zwitterion Preferred to a Quinoidal Structure: Its Reactivity Toward Organic and Inorganic Reagents. J Am Chem Soc. 2003;125(40):12246-56.
[31] Yang Q-Z, Siri O, Braunstein P. First transamination reactions for the one-pot synthesis of substituted zwitterionic quinones. Chem Commun. 2005(21):2660-2.
[32] Bonneau N, Chen G, Lachkar D, Boufridi A, Gallard J-F, Retailleau P, et al. An Unprecedented Blue Chromophore Found in Nature using a “Chemistry First” and Molecular Networking Approach: Discovery of Dactylocyanines A–H. Chem Eur J. 2017;23(58):14454-61.
[33] Ruiz AT, Bousquet MHE, Pascal S, Canard G, Mazan V, Elhabiri M, et al. Small Panchromatic and NIR Absorbers from Quinoid Zwitterions. Org Lett. 2020;22(20):7997-8001.

[34] Pascal S, Lavaud L, Azarias C, Canard G, Giorgi M, Jacquemin D, et al. Controlling the canonical/zwitterionic balance through intramolecular proton transfer: a strategy for vapochromism. Mater Chem Front. 2018;2(9):1618-25.
[35] Pascal S, Lavaud L, Azarias C, Varlot A, Canard G, Giorgi M, et al. Azacalixquinarenes: From Canonical to (Poly-)Zwitterionic Macrocycles. J Org Chem. 2019;84(3):1387-97.
[36] Liu Y, Duzhko VV, Page ZA, Emrick T, Russell TP. Conjugated Polymer Zwitterions: Efficient Interlayer Materials in Organic Electronics. Acc Chem Res. 2016;49(11):2478-88.
[37] Mahmood A, Yang C-S, Jang S, Routaboul L, Chang H, Ghisolfi A, et al. Tuning graphene transistors through ad hoc electrostatics induced by a nanometer-thick molecular underlayer. Nanoscale. 2019;11(42):19705-12.
[38] Luczak A, Ruiz AT, Pascal S, Adamski A, Jung J, Luszczynska B, et al. The Quinonoid Zwitterion Interlayer for the Improvement of Charge Carrier Mobility in Organic Field-Effect Transistors. Polymers. 2021;13(10):1567.
[39] Connelly NG, Geiger WE. Chemical Redox Agents for Organometallic Chemistry. Chem Rev. 1996;96(2):877-910.
[40] Lavaud L, Azarias C, Canard G, Pascal S, Galiana J, Giorgi M, et al. Fused bis-azacalixphyrin that reaches NIR-II absorptions. Chem Commun. 2020;56(6):896-9.
[41] Cho YJ, Yook KS, Lee JY. Cool and warm hybrid white organic light-emitting diode with blue delayed fluorescent emitter both as blue emitter and triplet host. Sci Rep. 2015;5(1):7859.
[42] M. J. Frisch et al. Gaussian 16, revision A.03, Wallignford, CT, USA, 2016.
[43] Adamo C, Barone V. Toward reliable density functional methods without adjustable parameters: The PBE0 model. J Chem Phys. 1999;110(13):6158-70.
[44] Yanai T, Tew DP, Handy NC. A new hybrid exchange–correlation functional using the Coulomb-attenuating method (CAM-B3LYP). Chem Phys Lett. 2004;393(1):51-7.
[45] Tomasi J, Mennucci B, Cammi R. Quantum Mechanical Continuum Solvation Models. Chem Rev. 2005;105(8):2999-3094.
[46] Le Bahers T, Adamo C, Ciofini I. A Qualitative Index of Spatial Extent in Charge-Transfer Excitations. J Chem Theory Comput. 2011;7(8):2498-506.
[47] Chen Z, Haddoub R, Mahé J, Marchand G, Jacquemin D, Andeme Edzang J, et al. N-Substituted Azacalixphyrins: Synthesis, Properties, and Self-Assembly. Chem Eur J. 2016;22(49):17820-32.
[48] Longevial J-F, Chen Z, Pascal S, Canard G, Jacquemin D, Siri O. Stabilization of a 12-π electrons diamino-benzoquinonediimine tautomer. Chem Commun. 2021;57(4):548-51.
[49] Hansch C, Leo A, Taft RW. A survey of Hammett substituent constants and resonance and field parameters. Chem Rev. 1991;91(2):165-95.
[50] Feldblum ES, Arkin IT. Strength of a bifurcated H bond. Proc Natl Acad Sci USA. 2014;111(11):4085-90.
[51] Chipanina NN, Oznobikhina LP, Sigalov MV, Shainyan BA. Intramolecular and intermolecular bifurcated hydrogen bonds in 2-pyrrolyl-7-hydroxy-2-methylidene-2,3-dihydro-1H-inden-1-one. J Phys Org Chem. 2019;32(4):e3924.